

DISCUSSION

Theoretical investigation of the time-dependent behaviour of rockfill

L. A. OLDECOP and E. E. ALONSO. (2007). *Géotechnique* **57**, No. 3, 289–301

Eulalio Juárez-Badillo, Graduate School of Engineering National University of Mexico

After reading this interesting paper the discussor was tempted to apply the theoretical equations given by the principle of natural proportionality to the experimental data contained in this paper and to gain additional experience on the common natural parameters corresponding to the crest settlement of different types of rockfill dams as well as to the one-dimensional compression tests on specimens of a rockfill-type material and the strain records with time obtained in each load step (under constant stress). Figs 14 to 16 show the theoretical equations: general time–settlement equation, general compressibility equation for soils and the general time–volume change equation for soils.

The general time–settlement equation reads (Juárez-Badillo, 2005)

$$S = \frac{S_T}{1 + (t/t^*)^{-\delta}} \tag{33}$$

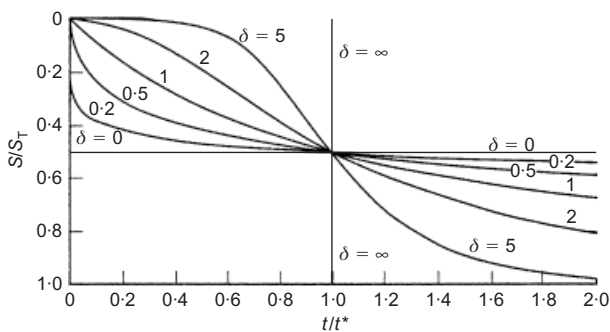


Fig. 14. Graphs of $\frac{S}{S_T} = \left[1 + \left(\frac{t}{t^*} \right)^{-\delta} \right]^{-1}$

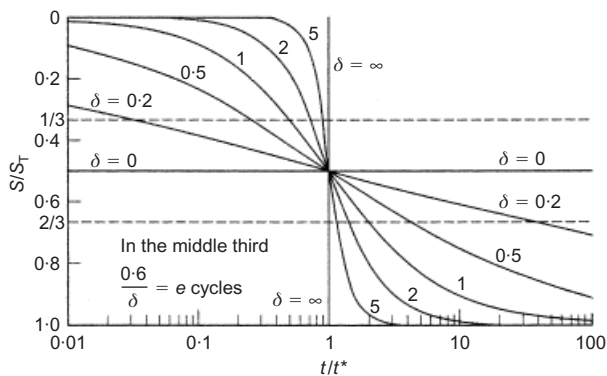


Fig. 15. Graphs of $\frac{S}{S_T} = \left[1 + \left(\frac{t}{t^*} \right)^{-\delta} \right]^{-1}$

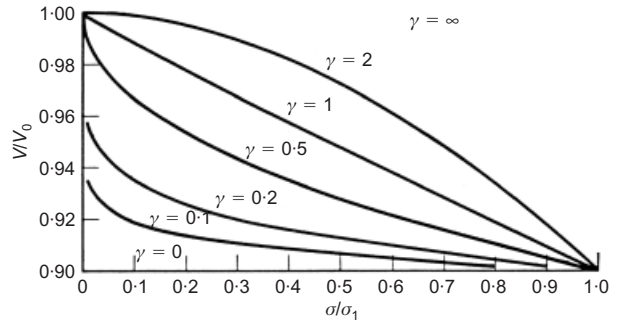


Fig. 16. Graphs of $\frac{(V_0/V)-1}{(V_0/V_1)-1} = \left(\frac{\sigma}{\sigma_1} \right)^\gamma$ for $\frac{V_1}{V_0}$

where S is the settlement at the time t , S_T is the total S at $t = \infty$, t^* is the characteristic t at $S = (1/2)S_T$ and δ is the fluidity coefficient.

Equation (33) was applied to various settlement records of Fig. 1. New Fig. 17 is the same original Fig. 1 with theoretical points included. The considered cases are indicated by an arrow and the theoretical natural parameters δ , t^* and S_T are included in Fig. 17 for each case. Fig. 14 was used for the determination of the parameters.

The general compressibility equation for soils in their first mechanical phase (unvirgin phase), before the second, more general, mechanical phase (virgin phase) reads (Juárez-Badillo, 1981)

$$\frac{V_0}{V} - 1 = \left(\frac{V_0}{V_1} - 1 \right) \left(\frac{\sigma}{\sigma_1} \right)^\gamma \tag{34}$$

where V is the volume at stress σ , $V_0 = V$ at $\sigma = 0$, (σ_1, V_1) is a known point and γ is the natural coefficient of compressibility.

Equation (34) may be written as

$$V = \frac{V_0}{1 + [(V_0/V_1) - 1](\sigma/\sigma_1)^\gamma} \tag{35}$$

If $\sigma^* = \sigma_1$ at $V_1 = V_0/2$, equation (35) may be written in the simpler and elegant form, where σ^* is known as the characteristic pressure

$$V = \frac{V_0}{1 + (\sigma/\sigma^*)^\gamma} \tag{36}$$

Figure 16 shows the graphs of equation (34) in a form very useful in practice. Here σ_1 is the pressure needed to reduce V_0 to $V_1 = 0.9V_0$. Then the compression curves for different values of γ are as presented in Fig. 16.

Equation (36) was applied to the four one-dimensional compression tests shown in Fig. 2. Fig. 18 is the same Fig. 2 with theoretical points included. The values of γ and σ^* were obtained using three experimental points on each

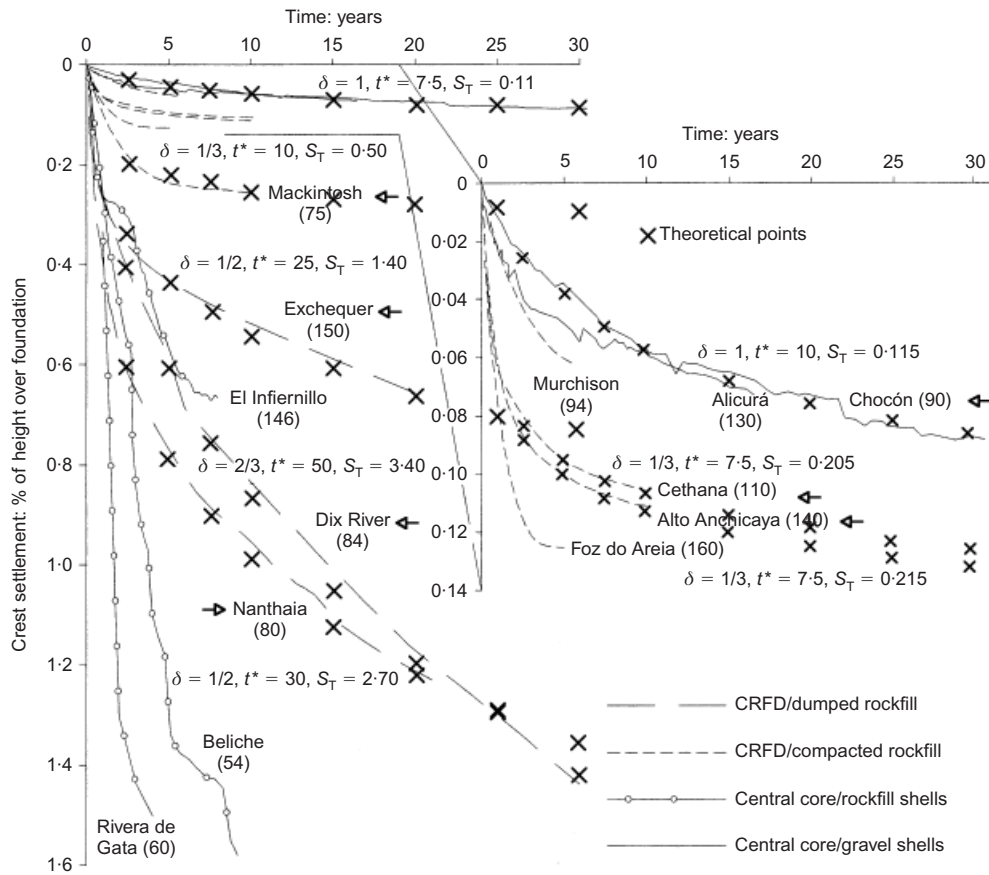


Fig. 17. Records of crest settlement of different types of rockfill dams built during the 20th century. Name (height in m) of the dam next to each curve. (Data sources: Marsal *et al.*, 1976; Sherard & Cooke, 1987; Soriano *et al.*, 1992; Naylor *et al.*, 1997)

experimental curve: the first point assuming $\epsilon = 0$ at $\sigma = 0$ (a better value for V_0 may be found as indicated in the Reference), the second point ϵ_2 at $\sigma_2 = 2.4$ MPa and the third point ϵ_3 at $\sigma_3 = 1.0$ MPa. The following equations used were (Juárez-Badillo, 1981)

$$\gamma = \frac{\log\{[(V_0/V_2) - 1]/[(V_0/V_3) - 1]\}}{\log(\sigma_2/\sigma_3)} \quad (37)$$

and

$$\left(\frac{\sigma^*}{\sigma_2}\right)^\gamma = \left(\frac{V_0}{V_2} - 1\right)^{-1} \quad (38)$$

The values of $\gamma = 1.01$, $\sigma^* = 17.7$ MPa for test 1 may somewhat be improved with a better value of V_0 , say $V_0 = 1.002$ ($\epsilon = -0.2\%$). Notice that the traditional bulk modulus K at $\sigma = 0$ is $K = \sigma^*$ for $\gamma = 1$ and $K = 0$ for $\gamma < 1$ and $K = \infty$ for $\gamma > 1$. See Fig. 16.

From Fig. 18 it appears that a good value for the natural coefficient of compressibility is $\gamma = 1.08$ for the four tests and that the characteristic pressure σ^* varies with the total suction as shown in Fig. 19

$$\sigma^* = 17.5 + \frac{1}{8}\Psi \quad (39)$$

The general time–volume change equation for soils (Juárez-Badillo, 1985) reads

$$\Delta V = \frac{(\Delta V)_T}{1 + (t/t^*)^{-\delta}} \quad (40)$$

where ΔV is the change in volume at time t , $(\Delta V)_T$ is the total ΔV at $t = \infty$, t^* = characteristic time at $\Delta V = (\Delta V)_T/2$ and δ is the corresponding fluidity coefficient. Observe the similitude of equation (40) with equation (33). Figs 14 and 15 are for the equation (40) if S and S_T are substituted by ΔV and $(\Delta V)_T$. Fig. 15 was used to obtain the parameters δ and t^* for the experimental data contained in Fig. 3. Fig. 20 is the same Fig. 3 with the experimental points included. Observe that the theoretical curve is practically a straight line in the middle third and it extends l cycles in the semi-log plot where $l = 0.6/\delta$ and therefore $\delta = 0.6/l$.

First, the cases 1.96 and 2.35 MPa were considered and it was found $\delta = 0.5$ and $t = 250$ min with $l = 1.2$ cycles. These values are shown in Fig. 20.

The cases 0.98, 0.60 and 0.41 MPa were subsequently considered using the same values of $\delta = 0.5$ and $t^* = 250$ min. The theoretical points appear in Fig. 20 with the symbol \times . For the case 0.98 MPa, however, it appears that $\delta = 0.20$ and $t^* = 50$ min and for the cases 0.60 and 0.41 MPa it appears that $\delta = 0.20$ and $t^* = 2$ min are better values. The corresponding theoretical points appear in Fig. 20 with the symbol $+$. Observing very carefully these last three cases it appears that $\delta = 0.5$ and $t^* = 250$ min are very good for times 0.01, 0.1 min and $t \geq 1000$ min, but for $t = 1, 10$ and 100 min it appears that after 0.1 min there were a ‘fluidity transition’ that changes the values of $\delta = 0.5$ and $t^* = 250$ min to $\delta = 0.20$ and $t^* = 50$ min for the case 0.98 MPa, and to $\delta = 0.20$ and $t^* = 2$ min for the cases 0.60 and 0.41 MPa considered. This is a very important point that the discussor suggests to the authors to revise. It would be good if $\delta = 0.5$ and $t^* = 250$ min were general

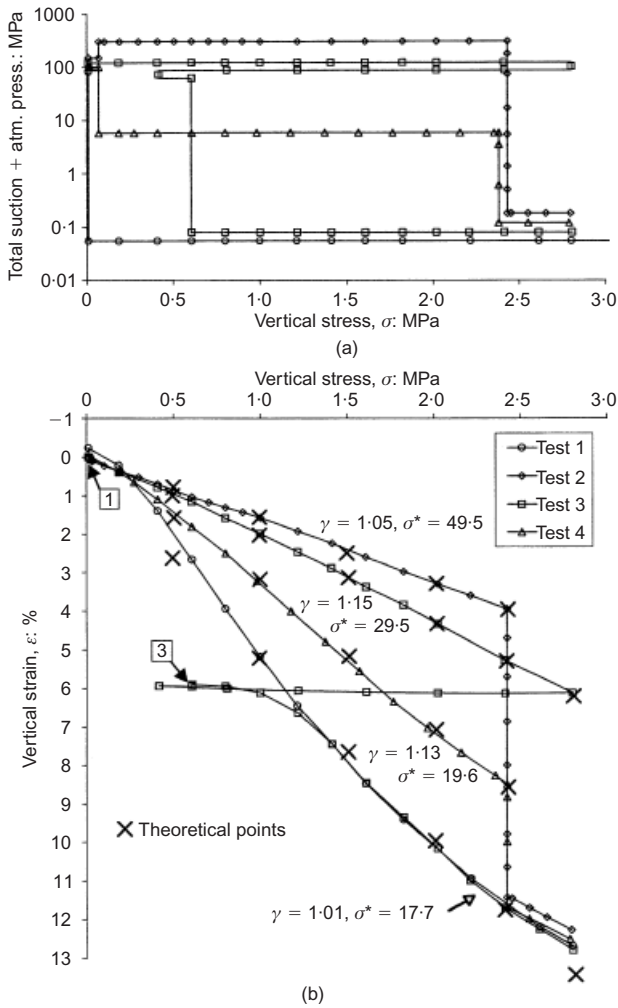


Fig. 18. One-dimensional compression tests with relative humidity control: (a) test paths in stress–suction space; (b) stress–strain curves with strain values measured at 1000 min after application of each load increment (Oldecop & Alonso, 2003)

values for all the cases considered in Fig. 20. The final theoretical points at $t = \infty$ have been marked in Fig. 20. These final values are also shown with the symbol $\rightarrow o$ in Fig. 21. In this figure, the symbol \times indicates the theoretical points at $t = 1000$ min for the four total suctions considered using the same values of γ and σ^* as in Fig. 18.

It can be concluded that the theoretical natural coefficients for the tests considered in Figs 18, 20 and 21 are $\gamma = 1.08$, σ^* given by the equation (39), Fig. 19, $\delta = 0.5$ and $t^* = 250$ min.

Authors' reply

We are grateful to the discussor for his interest in the paper and for his contribution in proposing alternative interpretations of the experimental data presented. The discussor applies a set of equations with the aim of reproducing the experimental and field data presented in the paper. The proposed equation (36), which is intended for the initial elastic phase of compression, is applied to the experimental data obtained in odometer tests, shown in Fig. 2. It should, however, be made clear that, in the authors' opinion, the data considered do not belong to the elastic compression phase of the studied material, but to virgin compression lines for different suction values. Although the tested rockfill specimens were prepared by tamping, a 'critical pressure' as mentioned in Juarez-Badillo (1981), dividing the initial elastic from the virgin compression phase (i.e. a preconsolidation stress) was not observed during compression of the specimens from zero up to 2.8 MPa (Oldecop & Alonso, 2001). In fact, the material experienced permanent strains from the very beginning of the loading path. The behaviour displayed by the specimens in Fig. 18 is very similar to the behaviour observed in odometer specimens of grainstone rockfill prepared with no compaction at all (Fig. 22), for which an initial elastic phase would not be expected to occur. On the basis of these observations, the authors interpret that each time a new rockfill specimen is built, either un-compacted or dynamically compacted, a virgin material is produced.

The model proposed by the discussor assumes that, for the virgin compression phase, the reference volume V_0 is infinite when the applied stress is nil (Juarez-Badillo, 1981). This feature has no physical sense for the experimental data presented in Figs 18 and 22. In both test series it is interpreted that the virgin compression lines start from the very beginning of the test, where specimens have, obviously, a finite volume.

The discussor queries the authors for reviewing the apparently anomalous behaviour of the experimental strain records of the odometer test 4 under vertical stresses 0.41, 0.6 and 0.98 MPa. In the central part of these records, the model proposed by the discussor substantially deviates from the experimental measurements. In the initial and final parts, however, the experimental records and the model predictions are in good agreement. The deviation arises mainly because of the sudden increments in strain at the beginning of records, which were systematically observed in low-stress loading steps. A physical explanation of this singular behaviour, different from the 'fluidity transition' suggested by the discussor, was proposed by Oldecop & Alonso (2002). The creep process, which follows each loading step, is interpreted as composed by two stages: the 'transient creep stage' and the 'normal creep stage'. During the transient creep stage, the time-dependent behaviour depends both on the loading conditions and on the previous loading history. The behaviour in the normal creep stage does not, however, depend on the loading history, but only on the applied stress and

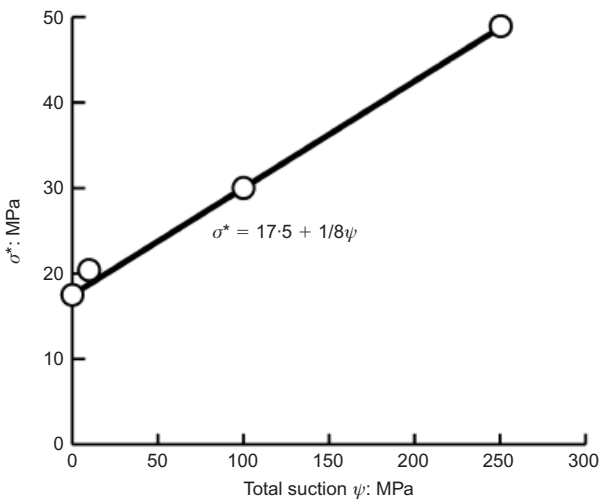


Fig. 19. Variation of σ^* with total suction ψ

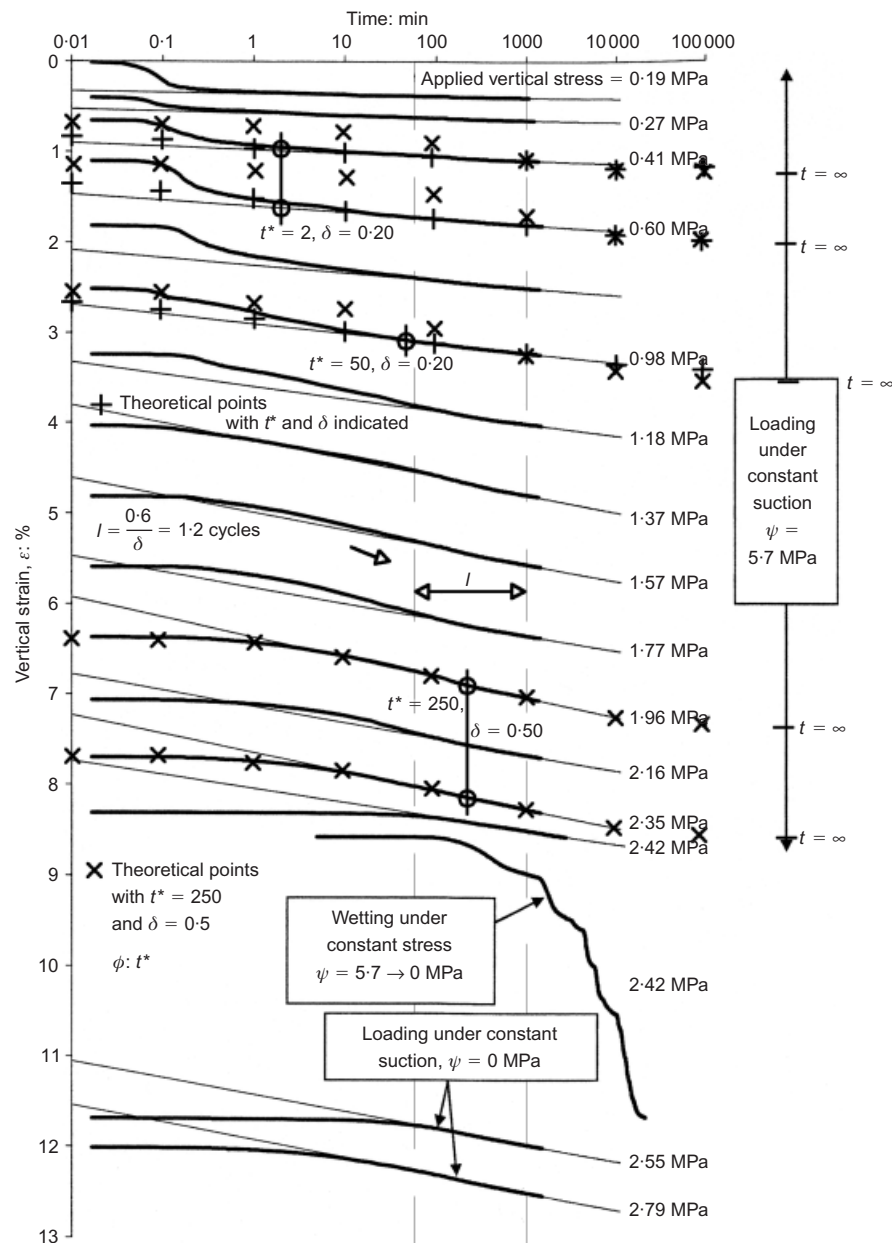


Fig. 20. Strain records obtained in each load step (under constant stress) of odometer test 4

total suction. It was suggested that cracks within the rock particles, which were propagated in previous loading steps, hold the memory of the recent loading history. A moment is, however, reached (the transition point between the referred first and second stage) when all those cracks are already broken and hence only virgin, non-previously propagated cracks are left in the material. All the loading memory was therefore erased and, upon that moment, the behaviour corresponds to a truly virgin material. As observed in the strain records in Fig. 20, the behaviour in the first stage is complex and difficult to predict, while in the second stage (say beyond 100 min after load increment application) the strain records follow a simple pattern, approaching straight strain-log(stress) lines. The slope and position of those lines seem to be completely determined by the stress and total suction applied to the material (Oldecop & Alonso, 2002).

The authors' research work related to rockfill materials,

presented in the reference paper and in some previous works (Chávez & Alonso, 2003; Oldecop & Alonso, 2001; 2002; 2003) is oriented towards the formulation of phenomenological constitutive equations capable of predicting the behaviour of rockfill under complex mechanical and environmental actions. Such conditions typically occur in engineering structures, such as embankments and dams, and moreover they may vary with time and combine in arbitrary loading sequences and cycles. Although the model proposed by the discussor reaches a relatively good approximation in fitting the experimental and field data, it does not seem possible for such a relatively simple model to predict or reproduce the behaviour of rockfill under loading-unloading-reloading paths combined with wetting and drying processes. It is the authors' belief that such a goal requires more sophisticated models, such as those formulated within the framework of hardening plasticity.

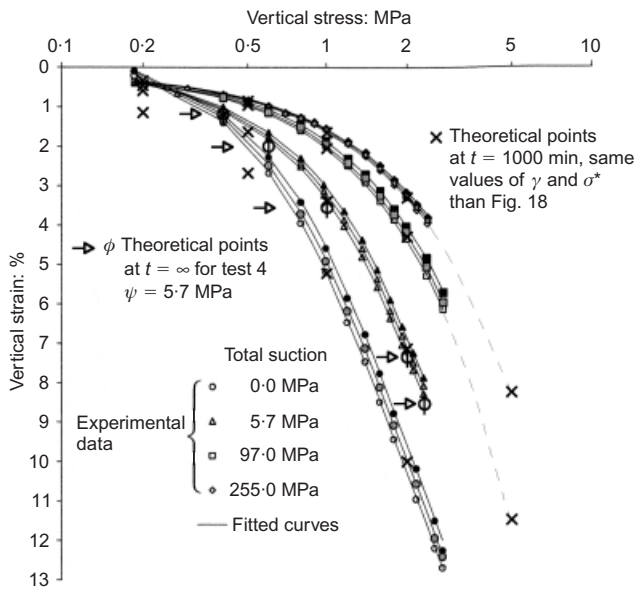


Fig. 21. Strain–stress curves measured at different time intervals after each load strip application: black symbols, $t^r = 10$ min; grey symbols, $t^r = 100$ min; open symbols, $t^r = 1000$ min

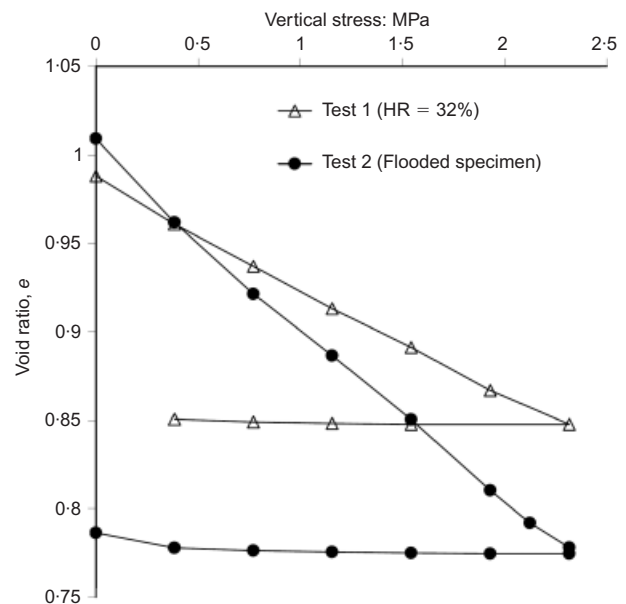


Fig. 22. Oedometer tests on grainstone rockfill (particle size: 30–50 mm, no compaction)

REFERENCES

- Chávez, C. & Alonso, E. E. (2003). A constitutive model for crushed granular aggregates which includes suction effects. *Soils & Foundations* **43**, No. 4, 215–227.
- Juárez-Badillo, E. (1981). General compressibility equation for soils. *Proc. 10th Int. Conf. Soil Mechanics and Foundation Engineering, Stockholm*, 171–178.
- Juárez-Badillo, E. (1985). General time volume change equation for soils. *Proc. 11th Int. Conf. Soil Mechanics and Foundation Engineering, San Francisco*, 519–530.

- Juárez-Badillo, E. (2005). Kansai International Airport, future settlements. *Proc. Int. 16th Int. Conf. Soil Mechanics and Geotechnical Engineering, Osaka*, **2**, 1053–1056.
- Oldecop, L. A. & Alonso, E. E. (2001). A model for rockfill compressibility. *Géotechnique* **51**, No. 2, 127–139.
- Oldecop, L. A. & Alonso, E. E. (2002). Fundamentals of rockfill time-dependent behaviour. *Proc. 3rd Int. Conf. Unsaturated Soils, Recife, Brazil*.
- Oldecop, L. A. & Alonso, E. E. (2003). Suction effects on rockfill compressibility. *Géotechnique* **53**, No. 2, 289–292.